Central European Journal of Energetic Materials
ISSN 1733-7178; e-ISSN 2353-1843


*Cent. Eur. J. Energ. Mater.* 2025, *22*(2): 141-165; DOI 10.22211/cejem/207449
Supporting Information is available in PDF-format, in colour, at:
https://ipo.lukasiewicz.gov.pl/wydawnictwa/cejem-woluminy/vol-22-nr-2/


***Research paper***

# Investigation of the Combustion and Radiometric Behaviour of Magnesium-Teflon-Viton (MTV) Decoy Flares by Partial Replacement of Magnesium

**Soujoy Debnath**[1,2,*], **Hitesh Kumar**[1], **Prashant Kulkarni**[1], **Sunil Jain**[1], **Shaibal Banerjee**[2]

[1] *High Energy Materials Research Laboratory, Sutarwadi, Pune, India*

[2] *Defence Institute of Advanced Technology, Girinagar, Pune, India*

* *E-mail:* sujoy.pac23@diat.ac.in

**Abstract:** Worldwide, studies are still being made to enhance the radiometric performance of the MTV composition, *i.e.* a composition of magnesium (Mg), polytetrafluoroethylene (PTFE, commonly called “teflon”) and Viton®, used in infrared (IR) decoy flares. In this study, the Mg fuel was replaced to modify the radiometric performance of the baseline MTV composition in terms of IR intensity and/or linear burn rate, along with the IR intensity ratio. To partially replace Mg, the fuels used were alloys: magnalium (Mg-aluminium (Al), 50:50) and boron Al ligature (BAL), a non-metal: silicon (Si), and organic fuels: 1,5-dinitronaphthalene (1,5-DNN) and 4-phenylazophenol (4-PAP). Composition batches of 100 g were prepared by replacing the Mg fuel, ranging from 5 to 25 wt.%, in the baseline MTV composition. The IR intensity in the 1.8-2.6 and 3-5 µm wavebands *versus* burn time was measured using a dual-band radiometer. The calorific value (Cal-Val), impact, friction and spark sensitivity measurements were obtained for all of the compositions. It was found that the IR intensities obtained were highest with the replacement by Magnalium, while those with organic fuels were the lowest. The maximum IR intensity was obtained at 5 wt.% replacement with Magnalium, which is 28.5% higher in the 1.8-2.6 µm range and 21.1% in the 3-5 µm range, and the linear burn rate was 9.8% lower than the baseline MTV composition. The IR intensity ratio was the lowest at 0.97 when 20% 4-PAP was partially replaced in the baseline MTV composition. The REAL thermochemical code was used to predict various equilibrium parameters of the MTV compositions. The thermochemical data was correlated with the spectral plot of the MTV compositions obtained by using an SR-5000N IR radiometer.

**Keywords:** MTV flare, fuel replacement, IR intensity, REAL thermochemical calculation, combustion

## 1 Introduction

To protect aircraft/helicopters from incoming IR-guided missiles, MTV compositions are widely used in IR decoy flares. The chemical reaction of the fuel and oxidiser in the composition gives a high heat of reaction, providing the desirable IR intensity in the mid-IR waveband. Excess Mg used in the MTV vaporises to produce MgO, to provide extra heat. MTV compositions are preferred over other pyrotechnic compositions due to their large energy output, low hygroscopicity, low dependence of burn rate on pressure and temperature and a relatively high degree of safety in preparation [1]. As the MTV composition delivers high IR intensity in the mid-IR region, various researchers have studied either the complete replacement of Mg and/or the use of alternative oxidisers along with additives. The main objective is to either increase the IR intensity in a specific waveband and/or to alter the burn rate.

Apart from chemical changes, various methods have also been used to enhance the performance of flare compositions. The performance parameters of compositions can be altered by physical means, such as altering the surface area by including grooves over the pellet surface *i.e.* altering the surface to volume ratio and/or altering the density [2]. In the particular case of MTV compositions, researchers have carried out various experiments (see [3-7]) to alter the dynamic performance of the composition for various performance parameters, their processing, emission behaviour and thermo-chemical and kinetics evaluation (see [8-11]). Yarrington *et al.* [12] have studied the combustion behaviour and pressure dependence of the burn rates of Si- and Al-based systems in Teflon®/Viton® mixtures and compared them with reported baseline MTV results. Studies, *e.g.* [13], have also been made to observe the effect of Al-Mg alloys with different Mg/Al ratios on the burning rate, combustion products, radiation intensity and specific radiation energy of Al-Mg/PTFE infrared compositions.

Toan and Cam [14] have studied the effect of Mg-Al alloy powder (*i.e.* the particle size and the composition) on the combustion and the infrared emission characteristics of pyrotechnic composition based on Mg-Al alloy, Teflon® and

Viton®. Also Elbasuney *et al.* [15] carried out studies with graphite particles of 100 μm size, with different reactive metal fuels including Mg, Al and Mg-Al alloy. It was observed that an increase in spectral intensity was obtained as compared to the baseline MTV compositions. Nguyen *et al.* [16] conducted studies to analyse the effects of iron(III) oxide nanoparticles on the burning characteristics *i.e.* the heat of combustion, the burning rate and the infrared radiance of the pyrotechnic composition based on MTV. Different flare formulations were studied based on Al as fuel, Teflon® as oxidiser and Viton® as a binder (with fuel percentages from 40 to 70%) [17]. The spectral performance of the developed formulations was evaluated for the thermal signature of the aircraft jet engine using a spectrophotometer.

A literature survey gave various attempts to alter the radiometric performance of MTV compositions by various methods, such as replacement of Mg, incorporation of additives and altering the stoichiometry of the composition. In the present study, in order to improve the IR intensity and reduce the burn rate, partial replacement of Mg was attempted with alloys, non-metals and organic fuels. The partial replacement was expected to either enhance the Calorific Value (Cal-Val) and/or introduce species into the combustion zone to increase the emissivity in the mid-IR waveband. According to [18], the IR intensity in the waveband of interest is related to the mass burn rate, emissivity of the combustion zone and the Cal-Val obtained from the composition. The latter can be determined using Equation 1.

$$I = m.\frac{1}{4\pi} H_c \, F_{\lambda,\mathrm{T}} \epsilon_{\lambda,\mathrm{T}} \tag{1}$$

where $I$ is the IR intensity (in W/sr) in the required waveband, $m$ is the mass consumption rate (in g/s), $H_c$ is the calorific value of the flare composition (in J/g),  is the fraction of total radiation in the band of interest and is the average emissivity of the combustion zone of the composition. A computational model was developed by Debnath *et al.* [19] to plot the IR intensity *versus* the burn time of the compositions consolidated in various flare configurations using Equation 1 and integrating it with the shrinking core model.

The REAL thermochemical code was used to predict the various species formed and the equilibrium parameters [20]. The values of the enthalpy of formation of various chemicals utilised in the MTV compositions were derived from the User's Manual for ICT-Thermodynamic [21-23]. Spectral plots of the compositions were obtained using a Spectroradiometer to correlate with the REAL calculations.

# 2 Materials and Methods

## 2.1 Materials

Spherical Mg powder had a particle size of <60 µm. Teflon® powder had an average particle size of 450-550 µm. Magnalium (Al:Mg = 50:50) was a fine powder with an average particle size of <60 µm. Magnalium was procured from MEPCO (Madurai) with an average particle size of 2-5µm. BAL powder having a composition of >79 wt.% boron, >12 wt.% Al and >1.5 wt.% Mg, was manufactured in our laboratory. The melting point of BAL could not be determined due to its very high melting point. Si powder had a purity of >99 wt.% with an average particle size of <15 µm. Both 1,5-DNN and 4-PAP were fine powders having particle size <10 µm. Si, 1,5-dinitronaphthalene (1,5-DNN) and 4-phenylazophenol (4-PAP) were procured from Alfa Aesar. The physical properties of these various chemicals are listed in Table 1.

**Table 1.** Physical properties of the chemicals used for flare compositions

| Chemicals | Formula | Molecular weight [g/mol] | Density [g/cm$^3$] | Melting point [°C] |
|---|---|---|---|---|
| Mg | Mg | 24.3 | 1.74 | 648.8 |
| Teflon® | $C_2F_4$ | 100.0 | 2.14 | 328.0 |
| Viton® | $C_{10}H_7F_{13}$ | 374.1 | 1.85 | 82.0 |
| Magnalium | $Mg_{0.5}Al_{0.5}$ | 26.5 | 2.12 | 600.0 |
| BAL | $B_{0.8}Al_{0.2}$ | 12.9 | 2.47 | n.d. |
| Si | Si | 28.1 | 2.33 | 1412 |
| 1,5-DNN | $C_{10}H_6N_2O_4$ | 218.2 | 1.61 | 219.0 |
| 4-PAP | $C_{12}H_{10}N_2O$ | 198.2 | 1.10 | 152.0 |

## 2.2 Processing of MTV compositions

The chemicals used were initially tested in-house for acceptance as per their material specifications. The baseline MTV composition consisted of 50 wt.% Mg, 45 wt.% Teflon® and 5 wt.% Viton®. The baseline composition is a standard MTV composition having an excess quantity of Mg. Excess Mg is generally used in such compositions as excess Mg vaporises to react with the atmospheric oxygen to provide additional energy, which contributes to an increase in IR intensity in the mid-IR waveband. 100g of the baseline MTV composition was prepared by manually coating the Mg powder with a slurry of Viton®. Viton® was gelled overnight in acetone before the coating operation. The coated Mg was partially air-dried for 15 min in an Al tray and granulated by passing through an 8 BSS sieve. The coating of Mg was done to avoid direct contact of atmospheric moisture with Mg, as Mg is known to degrade upon long-term exposure to moisture. The partially dried mixture was mixed manually with a weighed quantity of Teflon®. The mixture was then passed through an 8 BSS sieve three times. The composition was dried overnight on an Al tray.

The baseline MTV composition is designated as MTV1. The modified MTV compositions were prepared by replacement of 5 to 25 wt.%, *i.e.* 5 to 25 g, of the replacement fuels to the MTV1 composition. The MTV compositions obtained by replacement with 15 wt.% replacement fuels: Mg, BAL, Si, 1,5-DNN and 4-PAP to MTV1 composition are designated as MTV2, MTV3, MTV4, MTV5 and MTV6, respectively. The details of the studied compositions are given in Table 2.

A total of 25 batches of MTV2 to MTV6 compositions were prepared, along with one batch of the MTV1 composition. All the replacement fuels were premixed with Mg before coating with Viton®. After the evaporation of acetone from the sieved mix, the compositions were kept in an antistatic bag.

**Table 2.** Details of MTV1 to MTV6 compositions used in the study

<table>
<tr><th>Compositions</th><th>Fuel [wt.%]</th><th>Replacement fuel [wt.%]</th><th>Teflon® [wt.%]</th><th>Viton® [wt.%]</th></tr>
<tr><td>MTV1: Magnesium/Teflon/Viton</td><td>50</td><td>0</td><td rowspan="6">45</td><td rowspan="6">5</td></tr>
<tr><td>MTV2: Magnesium/Magnalium/Teflon/Viton</td><td rowspan="5">35</td><td rowspan="5">15</td></tr>
<tr><td>MTV3: Magnesium/BAL/Teflon/Viton</td></tr>
<tr><td>MTV4: Magnesium/Silicon/Teflon/Viton</td></tr>
<tr><td>MTV5: Magnesium/1,5-DNN/Teflon/Viton</td></tr>
<tr><td>MTV6: Magnesium/4-PAP/Teflon/Viton</td></tr>
</table>

## 2.3 Instrumentation

Cal-Val was measured using a Parr bomb calorimeter (Model: 6200), procured from Orbit Technologies. The bomb calorimeter was capable of measuring Cal-Val values of up to 8000 cal/g (33.44 kJ/g). A stainless steel crucible was used for holding the sample, and calibration was done using a benzoic acid sample. The spark sensitivity was carried out using in-house fabricated spark sensitivity measurement equipment with a working range of 4 to 5000 mJ. The impact sensitivity was carried out using a BAM Fall hammer apparatus with a drop weight of 2 kg and a maximum fall height of 170 cm. The friction sensitivity was carried out using a BAM friction apparatus, with a working range of weights of 0.5-36 kg. Both the impact and friction sensitivity apparatus were procured from OZM Research. An Orion dual-band IR radiometer from CI Systems Israel was used to simultaneously measure the IR intensities for a single flare in two channels when fired in a wind tunnel. The radiometer had a field of view of 12° with the InGaAs detector working in the range 1.0-2.5 µm and the PV-MCT detector working in the range 2.5-5.5 µm wavebands. A plot of spectral intensity versus wavelength was obtained using an SR-5000N Spectroradiometer. The measurement was carried in the range of 1.3-14.3 µm. However, the data presented here is for the waveband range of 1.3-5.0 µm. Both the radiometers were calibrated with a blackbody of temperature T = 1000 K (SR-2, CI Systems Israel, Cavity blackbody working up to 1200 °C).

## 2.4 Measurement methods

The Cal-Val was carried out using a bomb calorimeter pressurized with oxygen. 1g of the composition was taken in the bomb and ignited. The heat given out by the composition due to the reaction with oxygen was calculated as the Cal-Val value (in J/g).

20 mg of sample was used for each friction sensitivity test. The weights were rubbed against the composition kept over a surface of standard roughness, and non-ignition was reported by converting the weight into the value of force applied to the composition. The value (in N) of non-ignition of the sample for a minimum of three tests was reported.

The data for impact sensitivity was calculated using a statistical staircase method and was reported as the height (in cm) at which there was a probability of 50% of the times the composition ignited upon impact.

In the spark sensitivity measurement, the capacitor was charged before the start of the measurement and then discharged between two terminals, between which the composition was placed. The spark sensitivity value (in mJ) was reported as the energy at which the composition does not initiate repeatedly five times.

## 2.5 Consolidation of MTV composition

Before taking up the filling operation, the 20-mm diameter steel tube was lined on the inside with a paper liner, fixed with an epoxy solution. The series of explosive compositions were consolidated into each steel tube and consisted of the innermost layer of the MTV composition (10 g), above which the booster (0.5 g, 50:50 mix of the MTV composition and a fast-burning rate priming composition) was placed. The booster was a mixture that ensured that the flash from the priming composition initiated the booster, which in turn provided the flash to the MTV composition. The uppermost layer consisted of a priming composition (0.5g), which in this case was gunpowder (a mixture of sulfur, potassium nitrate and charcoal). Gunpowder can be easily initiated with the help of a squib, and hence it was used as the priming composition in this study. 6 steel tubes were filled for each MTV composition with replacement fuels. Using the MTV1 to MTV6 compositions, a total of 156 steel tubes were filled.

A 10-ton capacity hydraulic press having a cylindrical bore diameter of 80 mm and a downward speed of 5-20 mm/s was used to press the composition in a mould. The pelleting mould was cylindrical, having a height of 70 mm and an internal diameter of 20.2 mm. The hydraulic press was procured from Velan Engineering. The steel tube was placed in the pelleting mould, and the composition to be pressed was poured into the mould before the booster. The booster composition and the priming composition are then poured over the MTV composition. The plunger was placed over the composition. A load of 6 ton and a dwell time of 15 s was applied. The filled steel tube was extracted using an extraction mould. An electrical squib was assembled over the top layer of the explosive to initiate the flare using an electric current pulse.

The unfilled steel tube with a paper liner is shown in Figure 1(a). The pressing of the MTV composition in the steel tube using a hydraulic press is shown in Figure 1(b). The assembled flare is shown in Figure 1(c). The radiometric evaluation of each flare was done by placing the flare on a firing stand as shown in Figure 1(d). The electrical squib is a hot wire initiator with a resistance wire over which a heat-sensitive explosive is coated. Upon receiving the electrical impulse, the bridge wire is heated up and the explosive is initiated, which in turn initiates the top explosive layer of the flare. The flare fired inside the wind tunnel is shown in Figure 1(e). An exhaust fan placed at the back of the wind tunnel provided a wind velocity of 5-10 m/s, to drive away hot gases that might interfere with the radiometric measurement. The dual-band IR radiometer was placed at 40 m distance from the tunnel. Upon providing an electrical pulse to the squib, the flare fired, and the IR intensity versus burn time data was recorded. A similar methodology was used to measure the spectral intensity *versus* wavelength using a Spectroradiometer. IR efficiency (in W·s/g·sr) was calculated by multiplying the IR intensity by the burn time divided by the weight of the composition. The linear burn rate (in mm/s) was calculated by the height of the filling divided by the burn time obtained.

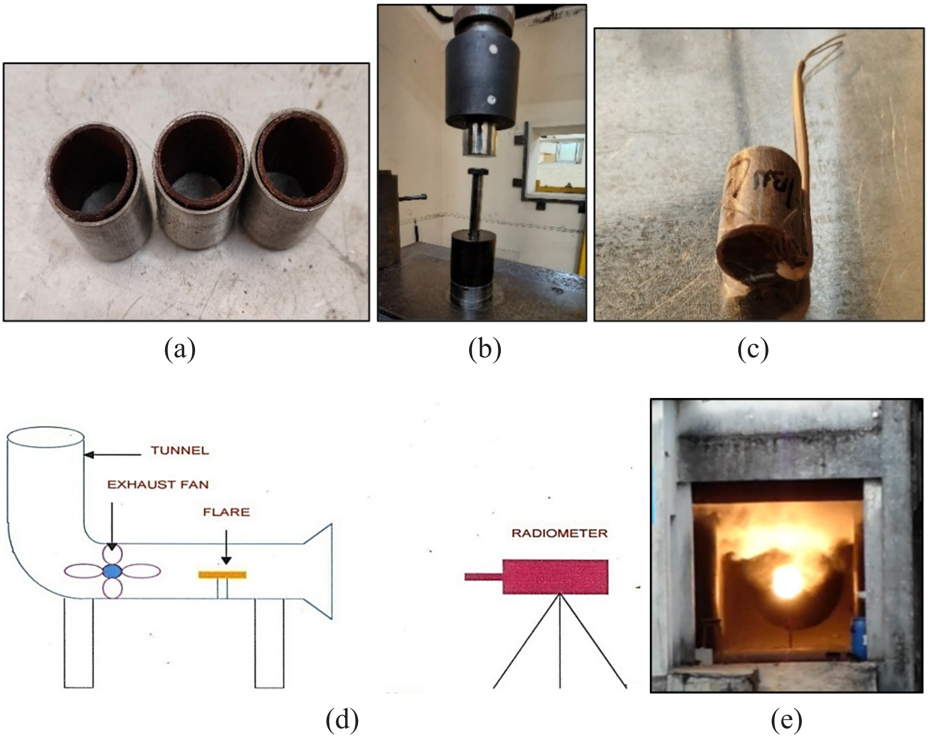


**Figure 1.** Preparation of samples and testing stand: paper-lined steel tubes (a), a hydraulic press used for composition pressing (b), steel tube filled and assembled with squib (c), measurement setup for radiometric performance using a dual-band radiometer/Spectroradiometer (d), and the flare fired in the wind tunnel (e)

# 3 Results and Discussions

## 3.1 Evaluation of MTV compositions

The radiometric performance of each composition was assessed by firing 3 flares after hot conditioning (+76 °C) for 3 h and 3 flares after cold conditioning (–46 °C) for 3 h. Simultaneous measurements in the 1.8-2.6 and 3-5 µm ranges were made using a dual-band radiometer. The data for each composition was calculated by averaging the data from firing of 3 flares after hot and 3 flares after cold conditioning The radiometric data for the MTV compositions are listed in Table 3. The radiometric plots obtained by the dual-band radiometer in the 1.8-2.6 and 3-5 µm ranges are shown in Figures 2 and 3, respectively. Figure 2(a) shows the plot of IR intensity for the MTV composition with partial fuel replacement (15 wt.%) *versus* the burn time obtained in the 1.8-2.6 μm range, while Figure 2(b) shows the plot of IR intensity of the MTV composition with partial fuel replacement (25 wt.%) *versus* the burn time obtained in the 1.8-2.6 μm range. Similarly, Figure 3(a) shows the plot of IR intensity of the MTV composition with replacement fuels (15 wt.%) *versus* the burn time obtained at 3-5 μm, while Figure 3(b) shows the plot of IR intensity of the MTV composition with replacement fuels (25 wt.%) *versus* the burn time obtained at 3-5 μm. Figure 4(a) shows the variation of the linear burn rate of the MTV composition *versus* wt.% of fuel replacement. Figure 4(b) shows the variation of the IR intensity of the MTV compositions *versus* their linear burn rates. Plot 4(a) helps in understanding the reaction mechanism by which replacement fuels enhance or reduce the burn rate. Plot 4(b) helps in finding the composition with enhanced IR intensity and with a lower burn rate. Cal-Val and sensitivity data for the MTV compositions are listed in Table 4.

**Table 3.** Radiometric data for MTV compositions

| Compositions | Fuel | Mg replaced by replacement fuel in MTV1 [wt.%] | IR intensity [W/sr] | | IR Efficiency [W·s/sr·g] | | IR Intensity Ratio [1.8-2.6]/[3-5] µm | Linear burn rate [mm/s] |
|---|---|---|---|---|---|---|---|---|
| | | | 1.8-2.6 µm | 3-5 µm | 1.8-2.6 µm | 3-5 µm | | 3-5µm |
| MTV1 | – | 0 | 287.3 | 239.1 | 179.0 | 149.0 | 1.38 | 3.86 |
| MTV2 | Magnalium | 5 | 369.3 | 289.6 | 239.0 | 183.0 | 1.28 | 3.48 |
| | | 10 | 347.1 | 279.9 | 225.0 | 183.00 | 1.22 | 3.23 |
| | | MTV2: 15 | 328.0 | 276.5 | 207.0 | 175.00 | 1.18 | 3.37 |
| | | 20 | 327.0 | 247.2 | 211.0 | 175.00 | 1.32 | 3.32 |
| | | 25 | 297.4 | 272.0 | 212.0 | 180.00 | 1.09 | 2.94 |
| MTV3 | BAL | 5 | 266.5 | 230.9 | 174.0 | 151.0 | 1.14 | 3.51 |
| | | 10 | 285.4 | 246.7 | 185.0 | 160.0 | 1.15 | 3.37 |
| | | MTV3: 15 | 279.7 | 247.7 | 198.0 | 175.0 | 1.12 | 3.05 |
| | | 20 | 291.6 | 251.5 | 222.0 | 191.0 | 1.16 | 2.94 |
| | | 25 | 259.4 | 220.5 | 219.0 | 187.0 | 1.17 | 2.64 |
| MTV4 | Si | 5 | 339.2 | 276.1 | 214.0 | 173.0 | 1.23 | 3.54 |
| | | 10 | 322.2 | 263.4 | 189.0 | 152.0 | 1.23 | 3.56 |
| | | MTV4: 15 | 302.9 | 251.3 | 186.0 | 154.0 | 1.21 | 3.52 |
| | | 20 | 289.6 | 247.2 | 184.0 | 157.0 | 1.17 | 3.39 |
| | | 25 | 284.1 | 229.8 | 187.0 | 151.0 | 1.23 | 3.21 |

**Table 3.** continuation

| Compositions | Fuel | Mg replaced by replacement fuels in MTV1 [wt.%] | IR intensity [W/sr] | | IR Efficiency [W·s/sr·g] | | IR Intensity Ratio [1.8-2.6]/[3-5] µm | Linear burn rate [mm/s] |
|---|---|---|---|---|---|---|---|---|
| | | | 1.8-2.6 µm | 3-5µm | 1.8-2.6 µm | 3-5 µm | | 3-5 µm |
| MTV5 | 1,5-DNN | 5 | 272.7 | 195.9 | 273.0 | 192.0 | 1.38 | 2.01 |
| | | 10 | 162.8 | 140.9 | 200.0 | 175.0 | 1.14 | 1.62 |
| | | MTV5: 15 | 178.9 | 156.2 | 260.0 | 235.0 | 1.14 | 1.34 |
| | | 20 | 155.0 | 132.9 | 247.0 | 236.0 | 1.17 | 1.14 |
| | | 25 | 101.4 | 95.7 | 239.0 | 232.0 | 1.06 | 0.84 |
| MTV6 | 4-PAP | 5 | 302.0 | 234.3 | 292.0 | 236.0 | 1.27 | 2.19 |
| | | 10 | 231.7 | 203.0 | 276.0 | 241.0 | 1.14 | 1.83 |
| | | MTV6: 15 | 138.0 | 125.9 | 228.0 | 208.0 | 1.12 | 1.36 |
| | | 20 | 104.0 | 108.4 | 199.0 | 225.0 | 0.97 | 1.07 |
| | | 25 | 88.5 | 87.3 | 217.0 | 214.0 | 1.01 | 0.94 |

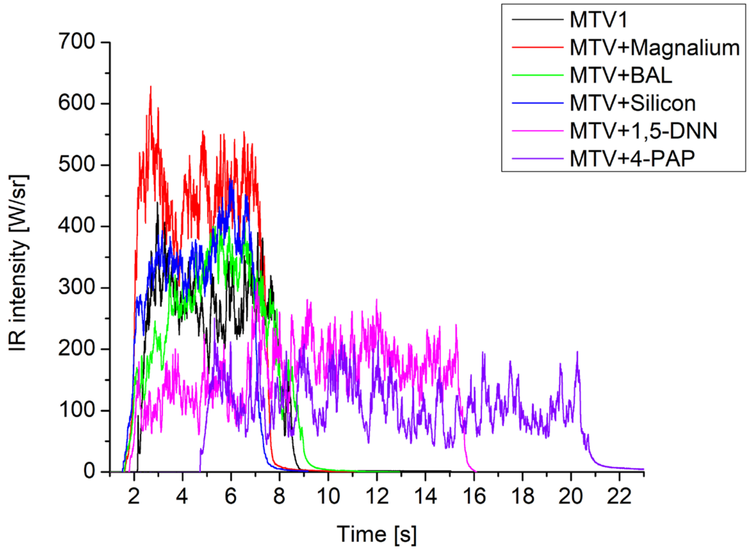


(a)

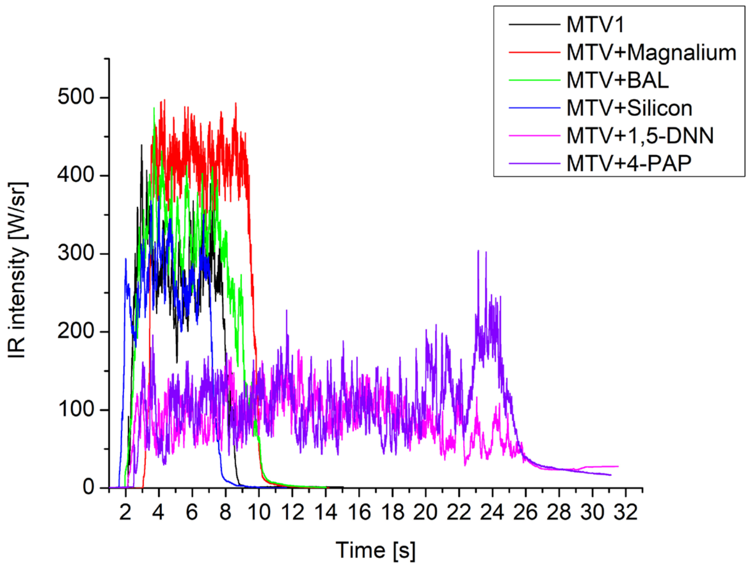


(b)

**Figure 2.** Plot of IR intensity *versus* time upon replacement of 15 wt.% (a) and 25 wt.% (b) of the fuel in the baseline MTV composition, measured by a dual-band radiometer in the 1.8-2.6 μm waveband

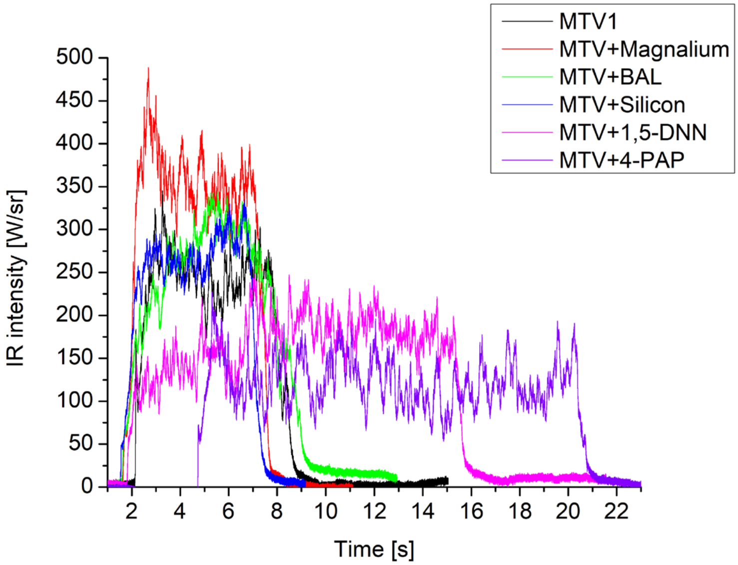


(a)

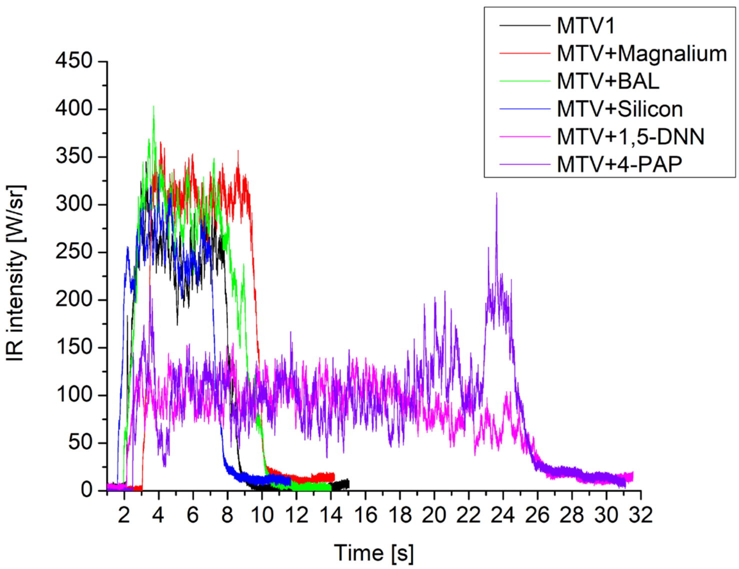


(b)

**Figure 3.** Plot of IR intensity *versus* time upon replacement of 15 wt.% (a) and 25 wt.% (b) of the fuel in the baseline MTV composition, measured by a dual-band radiometer in the 3-5 μm waveband

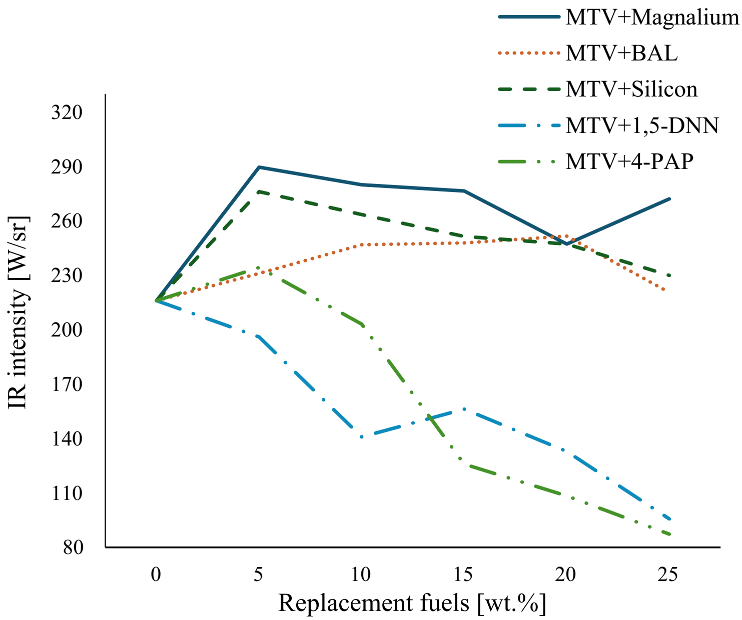


(a)

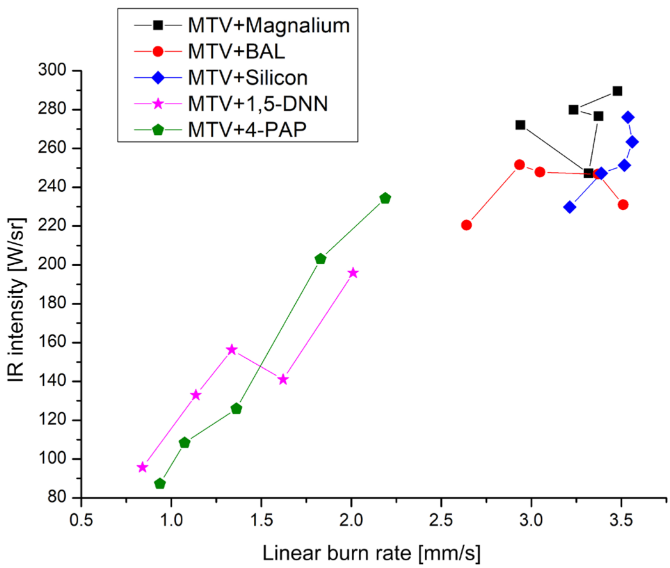


(b)

**Figure 4.** Plot of MTV compositions for: IR intensity *versus* (a) wt.% of replacement fuels and (b) linear burn rate

**Table 4.** Cal-Val and sensitivity data for MTV compositions

| Compositions | Fuel | Mg replaced by fuel in MTV1 [wt.%] | Impact sensitivity $H_{50}$ [cm] | Friction sensitivity: Not ignited up to [N] | Spark sensitivity: Not ignited up to [mJ] | Cal-Val [J/g] |
|---|---|---|---|---|---|---|
| MTV1 | – | 0 | 38.0 | 360 | 120.0 | 16092 |
| MTV2 | Magnalium | 15 | 35.0 | 360 | 54.0 | 20200 |
| MTV3 | BAL | 15 | 44.5 | 360 | 74.0 | 17347 |
| MTV4 | Si | 15 | 39.6 | 360 | 32.0 | 15913 |
| MTV5 | 1,5-DNN | 15 | 39.5 | 360 | 122.0 | 17790 |
| MTV6 | 4-PAP | 15 | > 100 cm | 360 | 138.0 | 17877 |

With the increase in quantities of magnalium, BAL and Si, the burn rate decreases while the IR intensity in both wavebands initially increases and thereafter decreases. With the increase in quantities of 1,5-DNN and 4-PAP, there is a decrease in IR intensity in both wavebands, with a drastic decrease in the burn rate. These plots can be utilised to obtain a composition for optimised performance parameters concerning IR intensities and burn rate.

The MTV1 composition's combustion reaction occurs in the absence of oxygen as in Equation 2. In the presence of oxygen, the carbon is oxidised to $CO_2$. Excess Mg is oxidised to magnesium oxide to provide extra energy.

$$6Mg + C_2F_4 + C_{10}H_7F_{13} \rightarrow 5MgF_2 + Mg + 12C + 7HF \tag{2}$$

## 3.2 Replacement with magnalium

The radiometric data suggest that, as compared to the baseline MTV composition, at 5 wt.% magnalium, the maximum IR intensity achieved at 1.8-2.6 µm is higher by 28.5% and at 3-5 µm is higher by 21.1%. As compared to the baseline MTV composition, the IR intensity ratio decreases by a maximum amount of 31.9% and the linear burn rate by 23.8%, both at 25 wt.% magnalium. Above 5 wt.% magnalium, the IR intensity in both wavebands decreases with an increase in magnalium content, but has a higher value than the baseline MTV composition, even at 25 wt.% replacement with magnalium. While the emissivity value [19] and the mass burn rate are lower than the baseline MTV composition, the higher Cal-Val of the MTV composition with magnalium leads to a higher IR intensity as per Equation 1. The reaction mechanism for MTV composition with magnalium in the absence of oxygen is proposed to be as in Equation 3. In the presence of oxygen, carbon is oxidised further to $CO_2$, and the hydrogen evolved is oxidised to water. Excess Mg is oxidised to magnesium oxide to release additional energy.

$$11Mg + C_2F_4 + 2C_{10}H_7F_{13} + 4Mg_{0.5}Al_{0.5} \rightarrow 12MgF_2 + Mg + 22C + 2AlF_3 + 7H_2 \quad (3)$$

## 3.3 Replacement with BAL

The radiometric data suggest that, as compared to the baseline MTV composition, at 20 wt.% BAL, the maximum IR intensity achieved at 1.8-2.6μm is higher by only 1.5% and at 3-5μm is higher by 5.2%. As compared to the baseline MTV composition, the IR intensity ratio was decreased by a maximum of 18.8% at 15 wt.% BAL and the linear burn rate by 31.6% at 25 wt.% BAL. Above 5 wt.% BAL, the IR intensity in both wavebands increases up to 20 wt.% BAL and decreases thereafter. While the emissivity value [19] and the mass burn rate are lower than the baseline MTV composition, the higher Cal-Val of the MTV composition with BAL leads to a higher IR intensity as per Equation 1. The reaction mechanism for MTV compositions with BAL in the absence of oxygen is proposed to be as in Equation 4. In the presence of oxygen, carbon is oxidised further to carbon dioxide, and the hydrogen evolved is oxidised to water. Excess Mg is oxidised to magnesium oxide to release additional energy.

$$13Mg + 7C_2F_4 + 2C_{10}H_7F_{13} + 10B_{0.8}Al_{0.2} \rightarrow 12MgF_2 + Mg + 34C + 2AlF_3 + 8BF_3 + 7H_2 \quad (4)$$

## 3.4 Replacement with Si

The radiometric data suggest that, as compared to the baseline MTV composition, at 5 wt.% Si, the maximum IR intensity achieved at 1.8-2.6 μm is higher by 18% and at 3-5 μm is higher by 15.5%. As compared to the baseline MTV composition, the IR intensity ratio decreases by a maximum amount of 15.2% at 20 wt.% Si and the linear burn rate by 16.8% at 25 wt.% Si. Above 5 wt.% Si, the IR intensity in both wavebands decreases up to 25 wt.% Si. While the emissivity value [19] and the mass burn rate are slightly lower than the baseline MTV composition, the Cal-Val of the MTV composition with Si is comparable to the baseline MTV composition. The MTV composition with Si produces a higher combustion temperature than the baseline MTV composition and hence produces a higher IR intensity in the lower waveband. The reaction mechanism for MTV composition with Si in the absence of oxygen is proposed to be as in Equation 5. In the presence of oxygen, carbon is oxidised further to $CO_2$, and the hydrogen evolved is oxidised to water. Excess Mg is oxidised to magnesium oxide to release additional energy.

$$16Mg + C_2F_4 + 2C_{10}H_7F_{13} + 2Si \rightarrow 15MgF_2 + Mg + 20C + 2SiC + 7H_2 \quad (5)$$

## 3.5 Replacement with 1,5-DNN

The radiometric data suggest that, as compared to the baseline MTV composition, the IR intensity at 1.8-2.6 and 3-5 µm continuously decreases up to 25% 1,5-DNN. The IR intensity ratio has decreased by a maximum amount of 23.2% and the linear burn rate by 78.2%, both at 25 wt.% 1,5-DNN. The reaction mechanism for MTV composition with 1,5-DNN in the absence of oxygen is proposed to be as in Equation 6. In the presence of oxygen, carbon is oxidised further to $CO_2$. Excess Mg is oxidised to magnesium oxide to release additional energy.

$$10Mg + C_2F_4 + 2C_{10}H_7F_{13} + C_{10}H_6N_2O_4 \rightarrow 9MgF_2 + Mg + 4H_2O + 32C + N_2 + 12HF \quad (6)$$

The combustion reaction of MTV with 1,5-DNN produces $H_2O$ and $CO_2$. These are selective emitters that emit in the mid-IR wavebands [24]. With the increase in 1,5-DNN content, the selective emitters in the combustion zone increase. However, as per Equation 1, the severe decrease in the mass burn rate reduces the IR intensity in both wavebands as compared to the baseline MTV composition. As the effect of burn rate reduction is more than the enhancement in the IR emission due to the increase in the emissivity of the various combustion products, there is an overall decrease in the IR intensities in both the wavebands with an increase in quantities of 1,5-DNN.

## 3.6 Replacement with 4-PAP

The radiometric data suggest that, as compared to the baseline MTV composition, the IR intensity at 1.8-2.6 and 3-5 µm continuously decreases up to 25% 4-PAP. The IR intensity ratio has decreased by a maximum amount of 29.7% at 20 wt.% 4-PAP and the linear burn rate by 75.6%, at 25 wt.% 4-PAP. The reaction mechanism for MTV composition with 4-PAP in the absence of oxygen is proposed to be as in Equation 7. In the presence of oxygen, carbon is oxidised further to $CO_2$. Excess Mg is oxidised to magnesium oxide to release additional energy.

$$5Mg + C_2F_4 + 2C_{10}H_7F_{13} + C_{12}H_{10}N_2O \rightarrow 4MgF_2 + Mg + 34C + H_2O + N_2 + 22HF \quad (7)$$

The combustion reaction of MTV with 4-PAP produces $H_2O$ and $CO_2$. These are selective emitters that emit in the mid-IR wavebands [24]. For similar reasons, as indicated for 1,5-DNN, there is an overall decrease in IR intensities in both wavebands with an increase in quantities of 4-PAP.

### 3.7 Cal-Val and sensitivity data of MTV compositions

The Cal-Val and sensitivity values were measured for MTV1 to MTV6 compositions. The results are listed in Table 3 in Section 3.1. It was observed that the addition of alloys such as magnalium and BAL increased the Cal-Val value, while the addition of Si decreased the calorific value compared to the baseline MTV composition. Amongst all the compositions, the magnalium-based composition recorded the highest Cal-Val value. This may be because magnalium has a lower melting point, and reacts with Teflon® to produce more heat as compared to Mg. Si has a higher melting point, which reduces the Cal-Val value, as heat is taken up to increase the temperature of Si up to its melting point. Although BAL has a higher melting point, the overall heat of reaction increases when boron and Al from BAL react with the fluorine in Teflon® to yield a higher Cal-Val value as compared to that of the baseline MTV composition. Although the melting points of organic fuels such as 1,5-DNN and 4-PAP are lower, their thermal decomposition leads to absorption of energy from the system, thus giving lower values of Cal-Val than the baseline MTV composition.

The impact sensitivity is lowest for the composition with 4-PAP (>100 cm) while it is highest for the composition with magnalium. The spark sensitivity is lowest for the MTV compositions with 4-PAP while it is highest for compositions with Si. All the compositions are safe for friction sensitivity and did not ignite even at 360 N force.

## 4 REAL Code: Thermo-chemical Calculations of MTV Compositions

The mass fractions for each chemical ingredient of the MTV compositions: MTV1 to MTV6 were used as input to the REAL thermo-chemical code. The equilibrium parameters, $H = 0$ kJ/kg and $P = 1$ atm were used for the calculations. The combustion species were predicted by the code on the assumption that the continuity, energy and momentum equations are one-dimensional, combustion is complete and adiabatic, the velocity of the combustion zone is zero, there is homogenous mixing of the species and no participation by atmospheric oxygen in the combustion zone. The enthalpy of formation of the chemical species was determined using the ICT thermochemical database [21-23]. The enthalpy of formation of Magnalium and BAL was found to be –96.68 and +1874 kJ/kg using the Miedema model calculator (see Zhang *et al.* [25]). The model is specifically used to calculate the formation enthalpies of various alloys using Miedema's theory. The various thermochemical equilibrium parameters are listed in Table 5.

**Table 5.** Prediction of species, their concentrations and equilibrium temperatures ($T_E$) using the REAL thermochemical code without the participation of oxygen in the combustion zone

| Composition | Species concentration [mass fraction] | | | | | | | | $T_E$ [°C] |
|---|---|---|---|---|---|---|---|---|---|
| | Mg | MgF | $MgF_2$ | $MgF_2$(c) | AlF | $AlF_2$ | $AlF_3$ | HF | |
| MTV1 | 0.229 | 0.119 | 0.370 | 0.150 | nd. | nd. | nd. | 0.004 | 2061 |
| MTV2 | 0.204 | 0.103 | 0.332 | 0.073 | 0.102 | 0.015 | 0.038 | nd. | 2036 |
| MTV3 | 0.227 | 0.071 | 0.179 | 0.044 | 0.061 | nd. | 0.012 | nd. | 1944 |
| MTV4 | 0.158 | 0.101 | 0.342 | nd. | nd. | nd. | nd. | nd. | 2111 |
| MTV5 | 0.099 | 0.113 | 0.477 | nd. | nd. | nd. | nd. | 0.035 | 2272 |
| MTV6 | 0.102 | 0.098 | 0.492 | nd. | nd. | nd. | nd. | 0.032 | 2118 |

| Composition | Species concentration [mass fraction] | | | | | | | | | $T_E$ [°C] |
|---|---|---|---|---|---|---|---|---|---|---|
| | BF | $BF_3$ | $B_4C$ | $SiF_2$ | AlF | SiC(c) | C(c) | CO | $N_2$ | |
| MTV1 | – | – | – | – | – | – | 0.124 | nd. | nd. | 2061 |
| MTV2 | – | – | – | – | – | – | 0.124 | nd. | nd. | 2036 |
| MTV3 | 0.026 | 0.170 | 0.080 | – | – | – | 0.106 | nd. | nd. | 1944 |
| MTV4 | – | – | – | 0.136 | 0.048 | 0.109 | 0.091 | nd. | nd. | 2111 |
| MTV5 | – | – | – | – | – | – | 0.171 | 0.077 | 0.018 | 2272 |
| MTV6 | – | – | – | – | – | – | 0.222 | 0.021 | 0.019 | 2118 |

nd.– no data

The correlation of equilibrium temperature, $T_E$, *versus* gaseous $MgF_2$ species obtained by REAL calculation is shown in Figure 5(a). The IR intensity in the 3-5 μm waveband measured by a dual-band radiometer *versus* the $T_E$ value obtained by REAL calculation is shown in Figure 5(b). The mass fraction of gaseous $MgF_2$ produced by the MTV1 composition is maximum (0.370). With the addition of magnalium, the gaseous $MgF_2$ decreased slightly, while the addition of BAL decreased the gaseous $MgF_2$ significantly. The $T_E$ value for the BAL-based composition was calculated to be lower than for both the magnalium-based and the baseline MTV compositions. A higher equilibrium temperature leads to higher gaseous $MgF_2$ species in the combustion zone.

The addition of Si leads to a slightly higher $T_E$, and the gaseous $MgF_2$ content was slightly lower as compared to that of the baseline MTV composition, and therefore the emissivity was decreased; however, due to the higher temperature, the IR intensities were increased. With the addition of organic fuels such as 1,5-DNN and 4-PAP, the $T_E$ values and gaseous $MgF_2$ values increased, along with the other selective emitters. However, the addition of organic fuels led to lower IR intensities in both wavebands than those from the baseline composition, due to the lower mass burn rate. Breaking down of the organic fuel to lower molecular weight species leads to a lowering of the linear burn rate and a decrease in IR intensities. The emission of selective emitters such as CO helps in decreasing the IR intensity ratio, as CO emits in the 3-5 µm waveband [24].

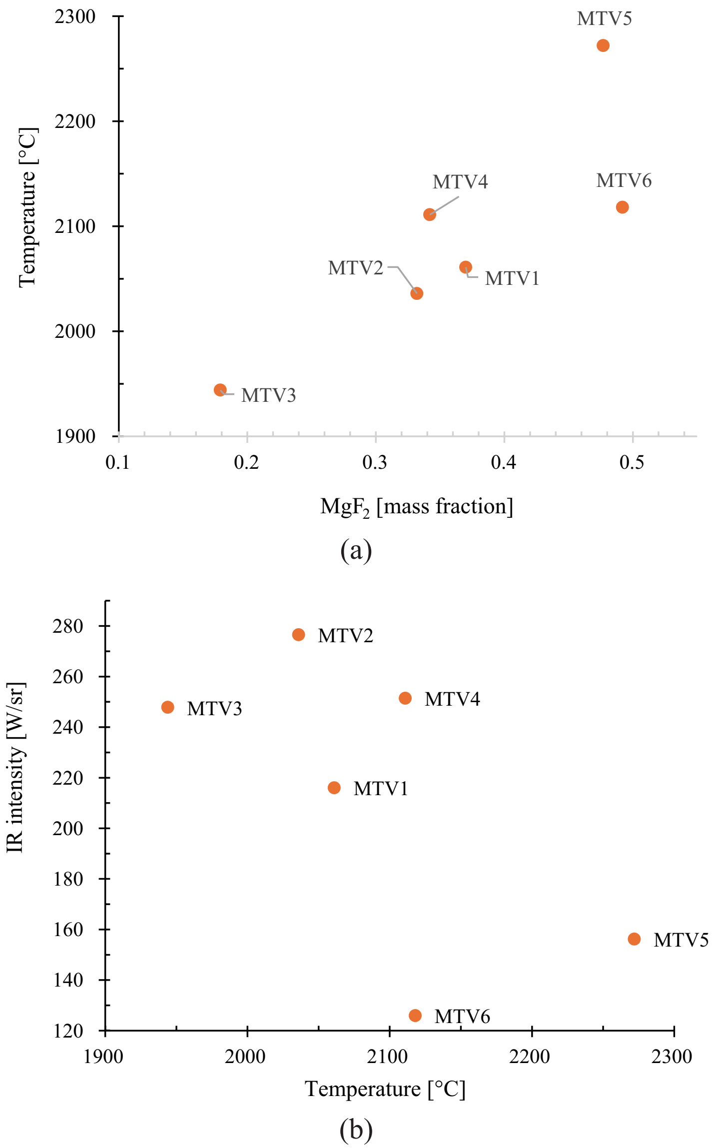


**Figure 5.** Equilibrium temperature *versus* (a) $MgF_2$ mass fraction and (b) IR intensity at 3-5 µm

## 5 Spectral Behaviour of MTV Compositions Using Spectroradiometer

The spectral behaviour of MTV1 to MTV6 compositions was measured using an SR5000N Spectroradiometer. The compositions were filled in 20 mm diameter steel tubes and fired in the wind tunnel setup. The plots of spectral intensity *versus* wavelength are shown in Figure 6. The measurements were carried out in the wavelength range of 1.3-5.0 µm. The plots show that the spectral intensity recorded in the entire wavelength spectrum was maximum for MTV2 and more than the baseline MTV composition. The MTV1 composition had a higher spectral intensity in the lower waveband in comparison to compositions MTV3 to MTV6. However, in the higher waveband, the MTV2 to MTV4 compositions demonstrated higher spectral intensity than the MTV1 composition. Although compositions MTV5 and MTV6 produce selective emitters such as CO and HF, in the entire waveband spectrum, the MTV1 composition was seen to have a higher spectral intensity. CO has a band strength of 250.36 $cm^2 \cdot atm^{-1}$ at 4.67 µm, while HF has a band strength of 250.36 $cm^2 \cdot atm^{-1}$ at 2.53 µm [24]. As the spectral intensity is a function of both emissivity and temperature, and since MTV5 and MTV6 have higher temperatures than the MTV1 composition, their lower spectral intensities show that the compositions must have a lower emissivity in their combustion zone.

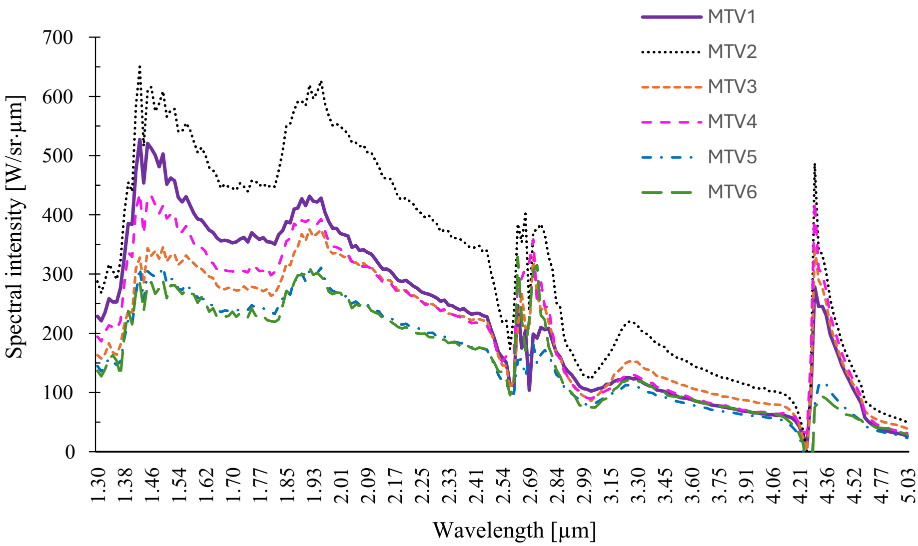


**Figure 6.** Spectral intensity *versus* wavelength using an SR-5000N Spectroradiometer

## 6 Conclusions

- In the present study, Mg fuel in MTV composition was partially replaced with up to 25 wt.% with replacement fuels consisting of alloys, non-metal and organic fuels. A literature survey carried out suggested that many researchers have worked on the complete replacement of Mg fuel in the MTV composition. However, in this study, a novel approach is made to partially replace Mg with fuels selected from alloys, non-metal and organic compounds. This was done in order to obtain a composition with a higher IR intensity and lower burn rate in comparison to the baseline MTV composition. A radiometric evaluation of various compositions suggests that appropriate amounts of alloys with lower melting points would enhance the IR intensities, together with a lower burn rate, as compared to the baseline MTV composition. Sensitivity, calorimetry and REAL calculations and spectral measurements revealed the combustion behaviour of these compositions.
- As compared to the baseline MTV composition, both magnalium and Si at 5 wt.% was found to give higher IR intensity in both 1.8-2.6 and 3-5µm wavebands, with a decrease in the linear burn rate and IR intensity ratio. However, as observed from Figure 4(b), the optimum composition for maximum IR intensity in both wavebands with a lower burn rate is the composition with 45 wt.% Mg, 5 wt.% magnalium, 45 wt.% Teflon® and 5 wt.% Viton®. High melting point alloys such as BAL do not show major improvements in the IR intensity in any of the wavebands. Literature [18] suggests that most operating flares reach effective intensity in less than 1 s and persist for less than 5 s. Therefore, a higher IR intensity with a lower burn rate should ensure that such compositions, when used in conventional flare format of either rectangular, square or circular cross-section, should provide a high IR intensity to decoy an incoming IR-guided missile and a higher burn time to ensure that the flare remains in the Field-of-View of the missile seeker for a longer time.
- The use of an organic fuel: 1,5-DNN leads to a decrease in the IR intensity in both wavebands, with the linear burn rate dropping by more than 75% at 25 wt.% for both 1,5-DNN and 4-PAP, with a decrease of the IR intensity ratio of more than 23%. While such fuels may not find use for the present requirement, they may find use in Multispectral IR flares, where a balance of IR intensity and IR intensity ratio is of greater importance.
- The sensitivity data for the compositions show that all compositions are insensitive towards friction. Organic fuel-based compositions are

comparatively insensitive towards impact, while alloys and non-metals show impact sensitivity similar to that of the baseline MTV composition. The spark sensitivity of alloys is higher compared to the baseline MTV composition, and with the addition of organic fuels, the compositions were found to be relatively insensitive towards spark. All compositions were found to be safe for large-scale processing.

- The addition of alloys increases the Calorific Value as compared to the baseline MTV composition due to the higher heat of reaction of fluorine with Al and boron. Due to the higher temperature of melting of Si, a decrease in Calorific Value is observed upon its addition. Due to the lower melting points of organic fuels such as 1,5-DNN and 4-PAP, a reduction in Calorific Value is observed due to heat absorption during the breakdown of the organic molecules.
- The thermochemical calculations using REAL code were performed for all compositions, giving an insight into their combustion behaviour and the various species and temperatures generated. The spectral behaviour of the MTV compositions using the Spectroradiometer was found to correlate to a large extent with the REAL calculations.

## Declaration of Competing Interest

The authors declare that they do not have any known competing financial interests or personal relationships that could have appeared to influence the work reported in this paper.

## Data Availability

The data related to the research shall be made available upon request.

## Acknowledgements

The authors are grateful to Dr. AP Dash, Director, High Energy Materials Research Laboratory, for permitting them to conduct the research work and for continuous guidance and support. The authors acknowledge the support and valuable guidance provided by Mr Shubhankar Roy, Technology Director of the Flares Division of this Laboratory. The authors acknowledge the help Mr Anand Pawar of the Instrumentation Division provided for carrying out the firing trials of the flares and providing the radiometric data. The efforts given to measure the Calorific Value, DSC and sensitivity data by the Quality Assurance and Reliability Division of the Laboratory are also acknowledged. Laboratory facilities and useful guidance provided by the Head of Department; Applied Chemistry of Defence Institute of Advanced Technology, is also acknowledged.

## References


[1] Titterton, D.H. Development of Infrared Countermeasure Technology and Systems. In: *Mid-Infrared Semiconductor Optoelectronics.* (Krier, A., Ed.) Springer, London, **2007**.

[2] Koch, E.C. Review of Pyrotechnic Aerial Infrared Decoys. *Propellants Explos. Pyrotech.* **2001**, *26*(1): 3-11; https://doi.org/10.1002/1521-4087(200101)26:1<3::AID-PREP3>3.0.CO;2-8.

[3] Kuwahara, T.; Toshinobu, O. Burning Rate of Mg/TF Pyrolants. *Proc. $18^{th}$ Int. Pyrotechnic Semin.* **1992**, pp. 539-548.

[4] Kuwahara, T.; Matsuo, S.; Shinozaki, N. Combustion and Sensitivity Characteristics of Mg/TF Pyrolants. Propellants Explosives and Pyrotechnics **2004**, *22*(4): 198-202: https://doi.org/10.1002/prep.19970220403.

[5] Miyake, A.; Kitoh, K.; Ogawa, T.; Watanabe, M.; Kazama, N.; Tsuji, S. Combustion Performance and Safety Evaluation of Mg/PTFE Pyrotechnic Compositions. *Proc. $19^{th}$ Int. Pyrotechnic Semin.* **1994**, pp. 124-134.

[6] Xue, W.; Gongpei, P.; Yi, L. The Influence of PTFE Effective Mass Flow Rate on 3-5μ Radiant Intensity in Mg/PTFE/$BaO_2$ Infrared Pyrotechnic Composition. *Proc. $24^{th}$ Int. Pyrotechnic Semin.* **1998**, pp. 607-612.

[7] Boulanger, R.; Souil, J.M.; Gillard, P.; Roux, M.; Espangnacq, A. Emission Spectral Computation for Pyrotechnic Applications. *Proc. $24^{th}$ Int. Pyrotechnic Semin.* **1998**, pp. 71-84.

[8] Deyong, L.V.; Smit, K.J. *A Theoretical Study on the Combustion of MTV Pyrotechnic Compositions.* DSTO Technical Report, MRL-TR-91-25, **1991**.

[9] Deyong, L.V.; Griffiths, T.T. The Use of Equilibrium and Kinetic Computer Programs to Study the Combustion of MTV Formulations. *Proc. $19^{th}$ Int. Pyrotechnic Semin.* **1994**, pp. 1-17.

[10] Brunet, L.; Forichon-Chaumet, N.; Lombard, J.M.; Espangnacq, A. Modelisation of Combustion Equilibria with Monte-Carlo Numerical Methods. *Propellants Explos. Pyrotech.* **1997**, *22*(6): 311-313; https://doi.org/10.1002/prep.19970220602.

[11] Webb, R. Possible Application for Computer Codes in the Development of Pyrotechnic Compositions. *J. Pyrotech.* **1998**, *7*: 74-75.

[12] Yarrington, C.D.; Son, S.F.; Foley, T.J. Combustion of Silicon/Teflon/Viton and Aluminum/Teflon/Viton Energetic Composites. *J. Propul. Power* **2010**, *26*(4): 734-743; https://doi.org/10.2514/1.46182.

[13] Wang, Y.K.; Zhang, M.X.; Liu, F.F.; Tang, J.S.; Zhu, C.G. Effect of Mg-Al Ratio on the Combustion and Infrared Radiation Properties of Al-Mg Alloy/PTFE Composition. *J. Phys.: Conf. Ser.* **2023**, *2478*(3) paper 032023; https://doi.org/10.1088/1742-6596/2478/3/032023.

[14] Toan, N.T.; Cam, N.N.T. Effects of Mg-Al Alloy Powder on the Combustion and Infrared Emission Characteristics of the Mg-Al/PTFE/Viton Composition. *Def. Sci. J.* **2020**, *70*(6): 590-595; https://doi.org/10.14429/dsj.70.15522.

[15] Elbasuney, S.; Elmotaz, A.A.; Sadek, M.A.; Yehia, M.; Tantawy, H. Superior Spectral Performance of Decoy Flares Compositions via the Inclusion of Graphite as a Black Body Emitter. *IOP Conf. Ser.: Mater. Sci. Eng. 975* **2020**, paper 012005, 1-13; https://doi.org/10.1088/1757-899X/975/1/012005.

[16] Nguyen, N.S.; Dam, Q.S.; Nguyen, V.T. Effects of Iron(III) Oxide Nanoparticles on the Burning Characteristics of the Pyrotechnic Composition for Infrared Emission Based on Magnesium-Teflon-Viton. *J. Sci. Tech.* **2023**, *1*(1): 65-76; https://doi.org/10.56651/lqdtu.jst.v1.n01.630.pce.
[17] Elsaidy, A.; Kassem, M.; Tantawy, H.; Elbasuney, S.; Gaber, Z.M. Infrared Spectra of Aluminium Fluorocarbon Polymer Compositions to Thermal Signature of Jet Engine. *Res. J. Mater. Sci.* **2018**, *6*(3): 189-197; https://doi.org/10.4172/2321-6212.1000232.
[18] Brune, N. Expendable Decoys. In: *The Infrared and Electro-Optical Systems Handbook, 7, Countermeasure Systems.* (Accetta, J.S.; Shumaker, D.L., Eds.) SPIE Optical Engineering Press, Bellingham, **1996**, pp. 289-321.
[19] Debnath, S.; Rej, P.; Kumar, H.; Jain, S.; Banerjee, S. A Computational Model for Prediction of IR Intensity and Burn Time of Magnesium-Teflon-Viton (MTV) Based Infrared (IR) Decoy Flare of Various Configurations. *J. Infrared Phys. Technol.* **2025**, *145* paper 105651; https://doi.org/10/1016/j.infrared.2024.105651.
[20] Belov, G.V. *Computer Simulations of Complex Chemical Equilibrium at High Pressure and Temperature, REAL Version 2.2.* Moscow, **1999**.
[21] Volk, F.; Bathell, H. *User's Manual for ICT-Thermodynamic Code, 1.* ICT-Report 14/88, Pfinztal, Germany, **1988**.
[22] Volk, F.; Bathell, H. *User's Manual for ICT-Thermodynamic Code, 2.* ICT-Report 1/91, Pfinztal Germany, **1991**.
[23] Volk, F.; Bathell, H. *User's Manual for ICT-Thermodynamic Code, 3.* ICT-Report 2/91, Pfinztal Germany, **1991**.
[24] Koch, E.-C. Pyrotechnic Countermeasures: II. Advanced Aerial Infrared Countermeasures, *Propellants Explos. Pyrotech.* **2006**, *31*(1): 3-19; https://doi.org/10.1002/prep.200600001.
[25] Zhang, R.F.; Zhang, S.H.; He, Z.J.; Jing, J.; Sheng, S.H. Miedema Calculator: A Thermodynamic Platform for Predicting Formation Enthalpies of Alloys within the Framework of Miedema's Theory. *Comput. Phys. Commun.* **2016**, *209*: 58-69; https://doi.org/10.1016/j.cpc.2016.08.013.

## CRediT authorship contribution statement

Soujoy Debnath: Conceptualisation, Methodology, Investigation, Formal analysis, Writing-original draft, Writing – review & editing.
Hitesh Kumar: Methodology, Investigation, Writing – review & editing.
Prashant Kulkarni: Methodology, Investigation.
Sunil Jain: Supervision, Visualization, Writing-review & editing.
Shaibal Banerjee: Supervision, Visualization, Resources, Writing-review & editing.

Submitted: February 9, 2025
Revised: June 23, 2025
First published online: June 30, 2025